Hindawi
International Journal of Geophysics
Volume 2022, Article ID 8451725, 13 pages
https://doi.org/10.1155/2022/8451725

Research Article

Subsurface Tectonic Inferences of the Adamawa Region of Cameroon from EMAG2 Magnetic Data

Kasi Njeudjang[1], **Justine Yandjimain**[2], **Apollinaire Bouba**[3], **Boris Merlain Djousse Kanouo**[4], **William Assatse Teikeu**[5], **Noël Djongyang**[6], **and Théophile Ndougsa-Mbarga**[2]

[1]*Department of Quality Industrial Safety and Environment, National Advanced School of Mines and Petroleum Industries, University of Maroua, P.O. Box 46, Maroua, Cameroon*
[2]*Department of Physics, Higher Teacher's Training College, University of Yaoundé I, P.O. Box 47, Yaoundé, Cameroon*
[3]*Department of Physics, Advanced Teacher's Training College, University of Maroua, P.O. Box: 46, Maroua, Cameroon*
[4]*Department of Rural Engineering, Faculty of Agronomy and Agricultural Sciences, University of Dschang, P.O. Box: 222, Dschang, Cameroon*
[5]*Laboratory of Geophysics and Geoexploration, Department of Physics, University of Yaoundé I, P.O. Box 812, Yaoundé, Cameroon*
[6]*Department of Renewable Energy, National Advanced School of Engineering of Maroua, University of Maroua, P.O. Box 46, Maroua, Cameroon*

Correspondence should be addressed to Kasi Njeudjang; kasinj2006@yahoo.fr

Received 31 March 2022; Revised 11 August 2022; Accepted 5 September 2022; Published 27 September 2022

Academic Editor: Arkoprovo Biswas

The study area includes an area between 6° to 8°N and 11° to 15°E. Geologically, it belongs to Precambrian basement (granites, gneisses), Proterozoic, and Archean (volcanic) series, showing the main heat sources of Cameroon. The purpose of this study deals to analyze and interpret the EMAG2 magnetic data in the Adamawa area using various advanced processing techniques. Thus, the mapping and depth estimation of underground structures are realized. The analysis of aeromagnetic map of the reduction to equator (RTE) in Adamawa area reveals rapidly evolving subsurface geological presented its lithological and structural. In the same, the power spectrum-processing tool clearly emphasizes shallow and deep underground heat sources. Two magnetic source location methods (source parameter imaging and analytical signal) are used to characterize of the source. The estimated magnetic source depths from source parameter imaging (SPI) are between 0.3 km and 22 km. The analytical signal ranges from 0.2 km to 31 km. In addition, the comparative study of 2D magnetic modelling showed that the basement is affected by the faults in the main directions of N-S, NE-SW, NW-SE, and WNW-ESE. The resulting structural map based on the tectonic map of Adamawa magnetic basement is a document that can simplify future hydrological and geothermal exploration.

1. Introduction

The present work focuses on the Adamawa region of Cameroon. The study area is an important morpho-tectonic structure located in the Pan-African fold zone in Central Africa [1], commonly known as Adamawa Yade Domain in Cameroon (AYD) [2]. It is believed that due to the reactivation of the Precambrian faults passing through the area, its uplift began in the Upper Cretaceous and expanded in the tertiary, like Darfur in Sudan, Tibesti in Chadian Sahara, Hoggar in the Algerian Sahara, or the "Rift Valleys" in East Africa. Adamawa is one of the African uplifts related to intraplate volcanism. Geophysical studies conducted in the area have revealed the source of hydrothermal solution, mineralization, and its relationship with other geological phenomena such as lithospheric thinning, tectonics, and

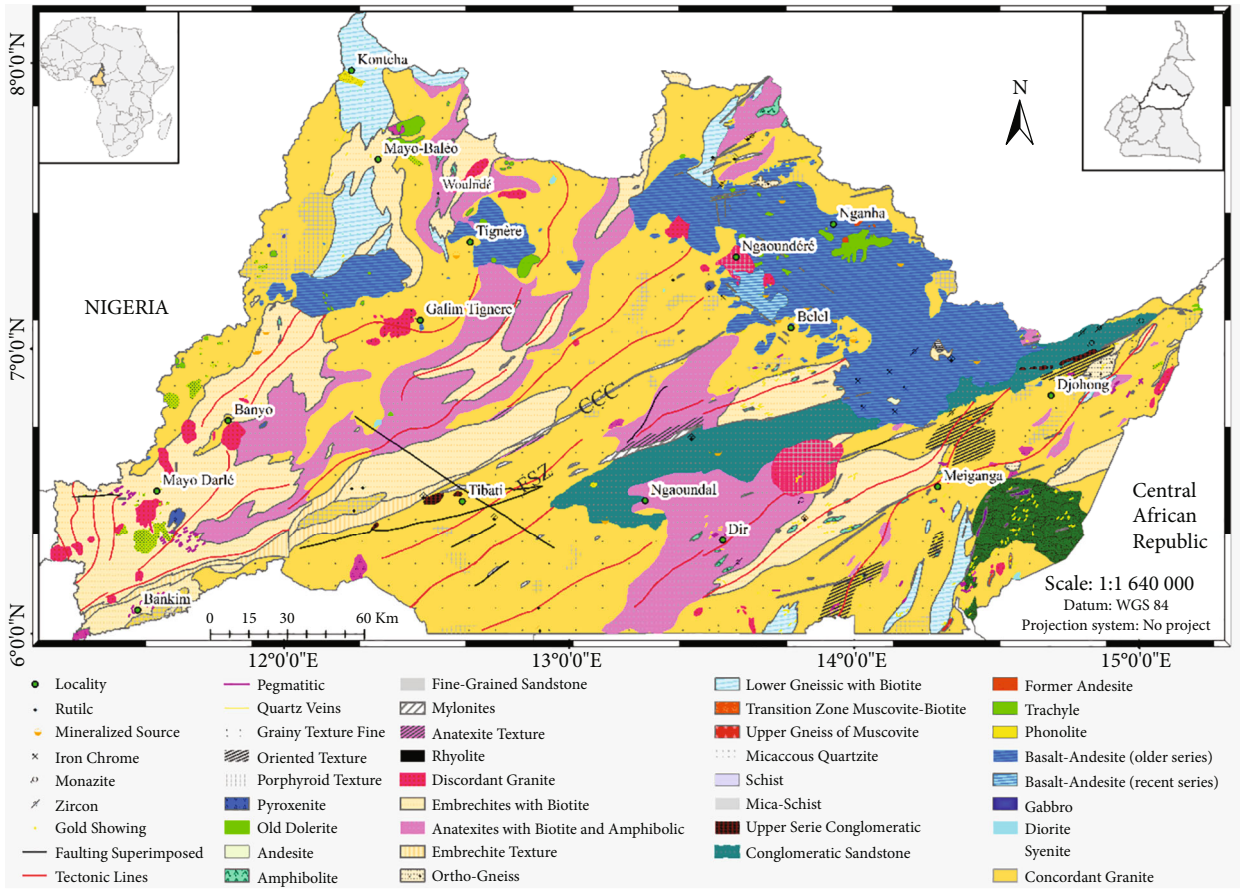

Figure 1: Geological map of Adamawa area (modified from [4, 22, 28]).

volcanism [3–8]. Geothermal activities are mainly prominent in the eruption center, especially in the Mount Cameroon, Adamawa region, and along the Cameroon Volcanic Line (CVL) (e.g., [9–12]).

Several authors have studied the internal structure of the Earth below the Cameroon Volcanic Line (e.g., [10, 13–17]). Therefore, on this region, Noutchogwe [18] highlights the correlation between the lineaments inferred from magnetic anomalies, thermo-mineral sources, and the hydrographic network. Some criteria for analyzing magnetic data are discussed in this paper. This paper also introduces some technical and software tools for processing and interpreting EMAG2 data to outline the characteristics of underground structures (deep and shallow). Therefore, the main objective of this work is to highlight the subsurface structure model. The model evaluation principle focuses on the spectrum at the reduced equator and the power curve of the regional residual separation. The source parameter images and analytical signal are used for quantitative depth estimation in addition to the interactive 2D magnetic modeling package run in the Geosoft program [19].

2. Geological Outline

Since the 1950s, the geological survey of Adamawa area has experienced three main stages [20, 21]. In the 1950s, after investigation and research, the geological map of Cameroon (Bureau of Mining and Geology) was established. This is followed by recent studies on the central domain of the Pan-African chain in Cameroon (e.g., [1, 22–29]) and finally on the Cameroon Line in Adamawa region [30–35]. These studies now allow the geological structure of Adamawa to be divided into two categories (Figure 1): bedrock and overlying formations.

The bedrock in this area includes Pan-African formations (sensu stricto) emplaced during orogeny and formations inherited from an older Pan-African structure. The reworked Paleoproterozoic formations are granulites composed of gneisses with high metamorphism aged at 2100 MA on the North Equatorial Pan-African chain of Cameroon [1, 22, 24]. These formations occur as cores (relics) in Pan-African formations [1, 24, 25, 28]. Granitoids, undifferentiated gneisses, and Lom series metasedimentary rocks constitute Pan-African formations "sensu stricto." Granitoids dominated by syn-tectonic granites are abundant below the Central Cameroonian Shear Fault Zone [24, 26, 29]. Undifferentiated gneisses are mainly distributed in the west of the area. Lom series metasedimentary rocks are composed of volcano-sedimentary and graphitic schists, quartzites, and micaschists [22, 36]. This series rests in discordance on the granito-gneissic basement [22].

The cover formation is a post Pan-African formation represented by Cretaceous sedimentary series and Cenozoic volcanic formations. The Cretaceous sedimentary series are the

filling sedimentation of Djerem-Mbéré basin. Djerem basin is composed of red clays and is located on the sandstone layers. In Mbéré trough, marls and clays are deposited on fine arkosic sandstones and conglomerates, partially covered by basanite flow [4, 37]. Many geological structures in Adamawa are mainly composed of basalts. These formations are related to volcanism along the Cameroon Line [38]. These rocks occur in the form of veins and, most importantly, in the form of very extensive but relatively thin flows that are strongly damaged by erosion and alteration. The emission types are fissural or Hawaiian, Vulcanian, and Strombolian [39]. The ages of lavas vary from Oligocene [40] to Mio-Pliocene [41, 42] [43] and Pleistocene [44] in the Ngaoundéré area. The volcanic rocks observed in this area are alkaline and related to continental rifts [45]. Related structures include the Cameroon Shear Zone, the South Adamawa Trough depression, and the Cameroon Volcanic Line.

3. Methodology and Data

This study is based on the magnetic field satellite data (Magsat) [46]. Adamawa and Central African shear zones (CASZ) have a large area of important negative anomaly. It crosses Africa from West to East and is about 1200 kilometers wide. The amplitude is 2 nT, extending longitudinally from ENE-WSW to E-W and from the Atlantic coast to about 30° E. Some satellite data show that the amplitude of this huge anomaly increases with the movement to low altitudes. Authors such as Regan et al. [47] and believe that this anomaly is a deep source anomaly of "de Bangui," while Dorbath et al. [5] attributed it to the lithospheric crust.

Since there is no single method to interpret magnetic data, many principles or parameters need to be considered when processing data. In fact, these parameters returned subsurface information's due to the magnetic signatures. They include the depth, shape, direction, and remanence of causal elements. In this study, magnetic data processing techniques (such as reduction to the equator) were performed using Geosoft mapping and processing system [19]. This reduction to the equator (RTE) data can be used for other survey tools to comprehensively infer the shape of underground structures. In addition, the residual filter, the depth estimation of source parameter images and analytical signal will lead to 2D profile modeling. The available RTE data are used to describe the characteristics of underground structures and effective trends related to these structures.

According to Nabighian [48] analytical signal is the three-dimensional (3D) vector where the absolute value of this signal is defined as the square root of the squared sum of the vertical and the two horizontal derivatives of the magnetic field. If M is the magnetic field, then the absolute value of this signal is given by:

$$|A(x,y)| = \sqrt{\left(\frac{\partial M}{\partial x}\right)^2 + \left(\frac{\partial M}{\partial y}\right)^2 + \left(\frac{\partial M}{\partial z}\right)^2}. \quad (1)$$

For effective modeling, a thorough knowledge of the geological structure of the basement of the study area is required; thus, certain parameters (position, depth, and contrast of susceptibility) of the source must be carried out starting from the knowledge of the structure. The 2D modeling is an appropriate method for modeling the base, seams, and semi-infinite contacts. The choice of the profile layout depends on the form and the position of the sources. On the residual map, the profiles are drawn perpendicularly to the anomalies using Geosoft's "GMSYS" module.

4. Results and Discussion

4.1. Total Magnetic Intensity (TMI) Anomaly. Figure 2 shows a series of positive (7.5 nT to 134 nT) and negative (121.2 nT to 0 nT) magnetic anomalies. These anomalies are polarities and have different form, wavelength and amplitudes, polarities, and ranges. All of these depend on underground characteristics as depths, sources, and components. It also reveals that most anomalies are arranged along the E-W direction with obvious and regular gradients, indicating that different tectonic forces in geological history have affected the area. Short wave and short amplitude negative anomalies were found in the SW and NE of the Adamawa region. These anomalies are caused by surface magnetism as highlight by Nnange [49]. The positive anomalies have long wave, and continuous amplitudes extend from Ngaoundéré to Kontcha and SE of Meiganga. The observed anomalies are round, elongated, and strongly graded oval contours.

Similarly, the comparison of the geological map of the region (Figure 1) and the magnetic field intensity map shows that there is a close correlation between geology and the variation of regional magnetic field intensity, which may be due to the different parameters of existing causal elements (magnetic rocks). Furthermore, Figure 2 shows high magnetic field intensity in Djohong, Kontcha, Mayo-Baléo, Meiganga, Nganha, Ngaoundéré, Tignère, and Woulndé. They are related to the high abundance of magmatic rocks (such as Basalts and Gabbros) of regional volcanism or the tectonics of the region [8].

The short wave anomalies in the SE and SW of the uplift axis can be lying to the influence of the shallow sources and the crustal [50]. These are being also due by the Cretaceous uplift in NE Cameroon [51]. The long wave anomalies are highlighting the solid formations in deep depths. Therefore, the result of this study are consistent as those of Nguiya [52], indicating the suppression of tilt effect and magnetic field declination; the shape and size of magnetic anomaly have changed slightly, showing an important discontinuity.

4.2. Reduction to the Equator Technique. Figure 3 shows that the pink, green, and magenta patches are located to the north and southeast. They reflect the high magnetic response. These are positive anomalies with magnetic values ranging from 1.9 nT to 126.9 nT, showing a NE-SW and NW-SE orientation. In addition, amplitude values between -85.9 nT and -2.7 nT indicates weak magnetic zones in the core of the investigation area. They are represented by the blue, green, and yellow colors indicating negative anomalies. The anomalies are usually of the NW-SE and NWW-SEE orientations. Figure 3 also shows a contact point in the

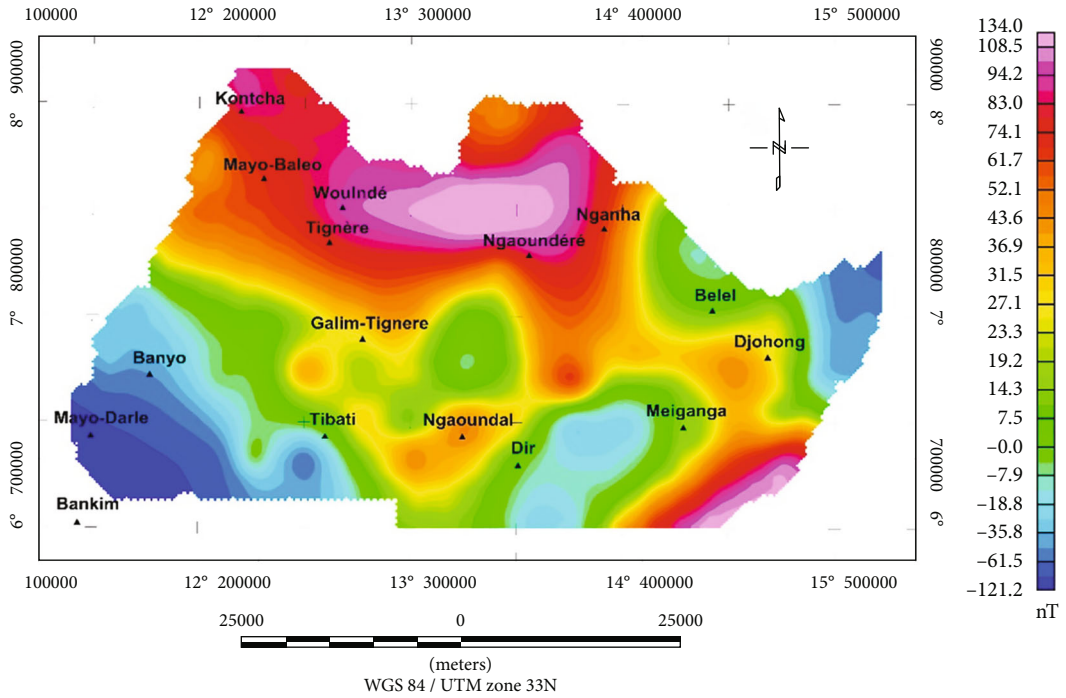

Figure 2: Anomaly map from total magnetic intensity (TMI) of Adamawa region.

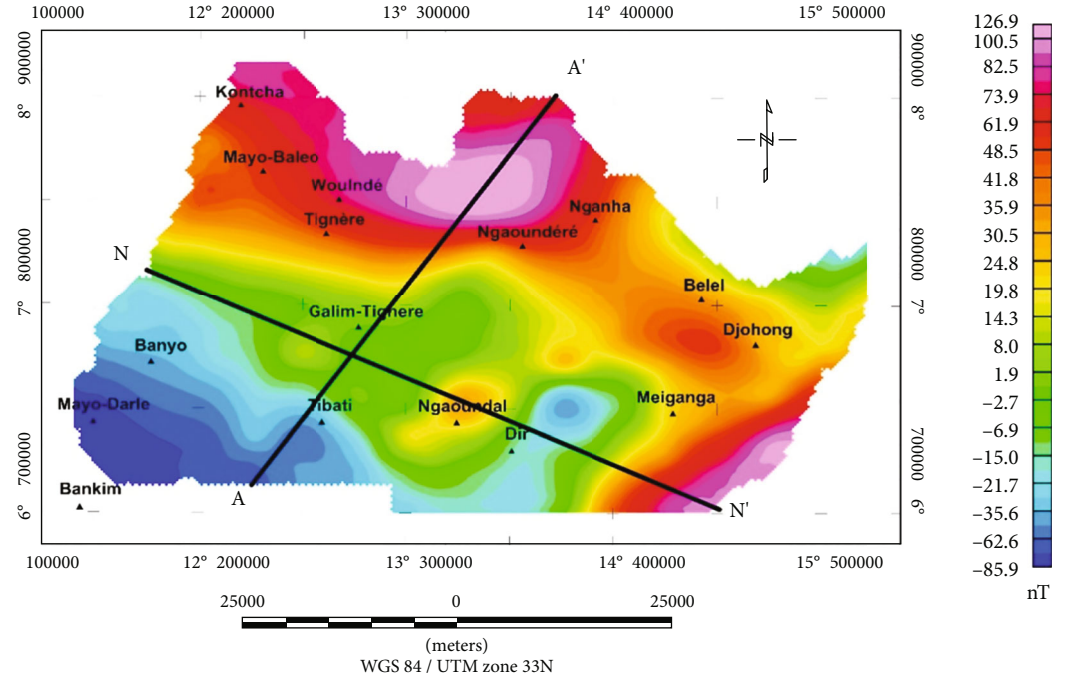

Figure 3: Reduced magnetic map at equator (RTE) illustrating location of 2D magnetic modeling profiles.

northern Adamawa region, distinguishing the high magnetic reply area from the weak magnetic reply area. This indicates that the degree of anomaly is directly proportional to the size of the causal bodies.

4.3. Regional-Residual Separation. This section uses radially average power spectrum filter (band-pass filtering) to obtain a residual magnetic anomaly by rejecting from the RTE, regional features of the magnetic anomaly field [53]. In this method, we firstly make the RTE grid periodic before any passage into the wave number domain by FFT (fast Fourier transformed). The second stage consists of finding by a trial and error procedure and the best wavelength combination that best enhance the regional/residual features of the magnetic field after the computation of the spectrum. The wavelengths cutoff are systematically adjusted until the regional

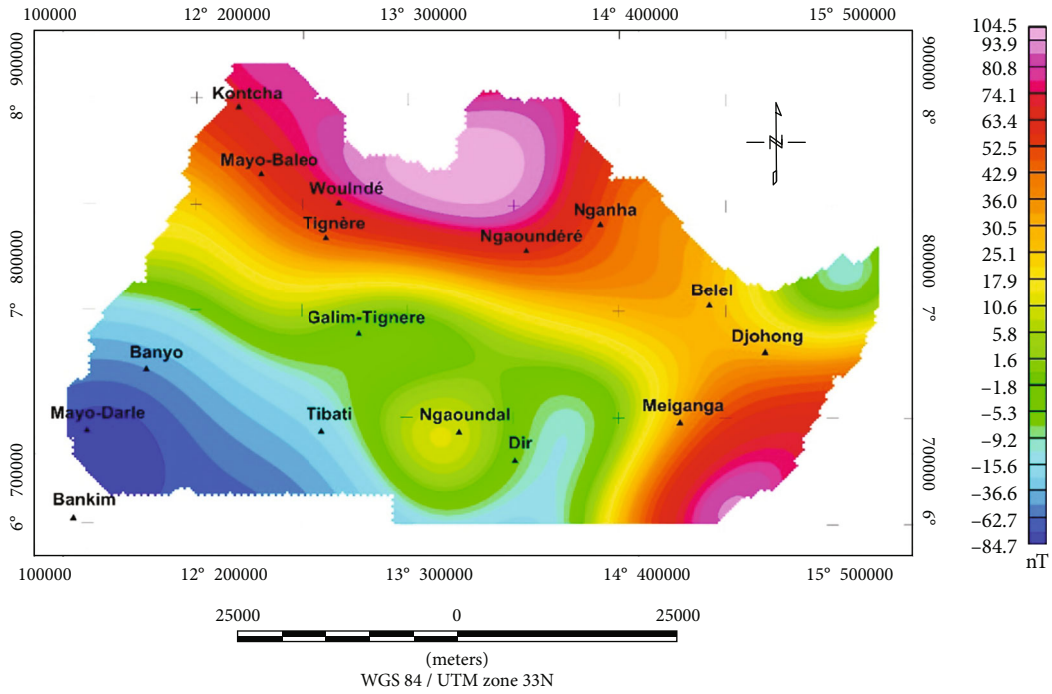

Figure 4: Regional magnetic anomaly map of Adamawa region.

and residual component of the magnetic field agrees with known geology of the region. Using the fast Fourier transform filtering (FFTFIL) program [19], the applied RTE correction contributes to an inclination of -10.98° and a declination of -0.91°. The last step is interpretation technique, in which different types of processing and filtering are performed on the RTE aeromagnetic map to improve the quality of data and separate the shallow source anomaly from the deep source anomaly.

4.3.1. Regional Magnetic Anomaly (RMA) Map. The RMA (Figure 4) highlights large wavelength and characterizes deep magnetic sources. Similarly, a detailed analysis of this map correlates with those has appeared in the RTE magnetic map (Figure 3), with lower amplitudes and frequencies. These structures are mainly near N-S and NW-SE. Positive anomalies are obviously related to the surrounding magnetic characteristics in Mayo Baléo, Woulndé, Tignère, Ngaoundéré, Kontcha, Nganha, Belel, Djohong, and Meiganga hot springs to varying degrees. These positive anomalies have great amplitudes ranging from 0 nT to 104.5 nT highlighting the formations due to high aimantation like ultrabasic intrusions. The negative anomalies have its amplitude between -84.7 nT and 0 nT. This last highlights the formations due to poor aimantation sources. They are also found in Mayo Darlé, Banyo, Tibati, and Dir areas.

4.3.2. Residual Magnetic Anomaly Map. The residual magnetic component map (Figure 5) shows discontinuous variations in magnetic contrast related to geological features and/or shallow bodies' features. In general, constitutive structures and/or respective depths of their sources may cause these changes. Some high amplitude magnetic anomalies have been found in Eocene ferruginous sandstone formations. They have E-W, ENE-WSW, and N-S orientations with magnetic values ranging from 0 nT to 31.6 nT. On the other hand, low amplitude magnetic anomalies are geologically related to the formation of Cretaceous sediments, ferruginous conglomerate, lateritic sandstone, grey clay, and ferruginous grey clay stones. Their amplitudes range from -31.1 nT to 0 nT and are NE-SW and N-S directions.

4.4. Spectral Analysis. Spectral analysis, also known as "power spectrum curve," is a technique based on fast Fourier transform filtering [54]. Figure 6 presents the radial average power spectrum calculated for RTE map. It presented three parts: the deep sources, shallow sources, and noise. The deep (or regional) sources are the first part with the frequency range 0.05 km^{-1} and joint to the high wavelengths represented on the RMA. The shallow (or residual) sources are the second part with the frequency range from 0.1 to 0.3 km^{-1} corresponding to short wavelengths. These wavelengths are represented on the RTE. The third part of the noise with a frequency is greater than 0.3 km^{-1}. The slope of the straight of both first parts is used to estimate the average depths of magnetic sources. The depths of 1.6 km are due to the regional sources, while the depths of 23 km are due to the residual sources (Figure 6).

4.5. Quantitative Interpretation. Quantitative interpretation involves numerical analysis functions applied to potential field data. Therefore, it helps to determine various geological constraints including source location, shape, depth, thickness, and composition. Three methods are used in this study.

4.5.1. Source Parameter Image. Source parameter imaging (SPI) is a method to calculate source depths using magnetic

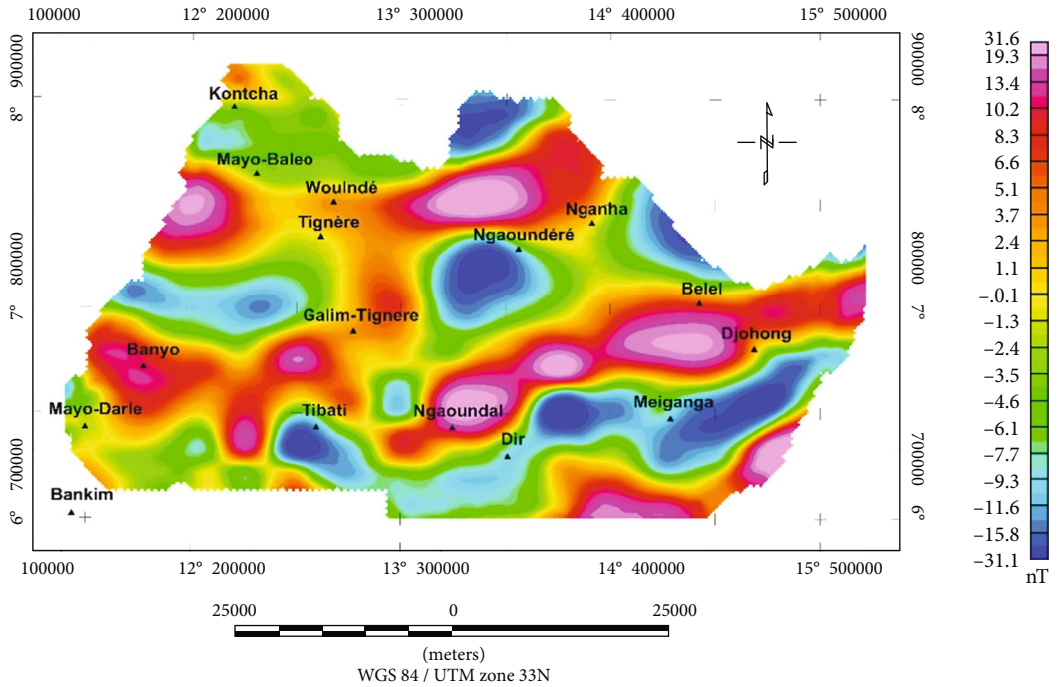

Figure 5: Residual magnetic anomaly map of the study area.

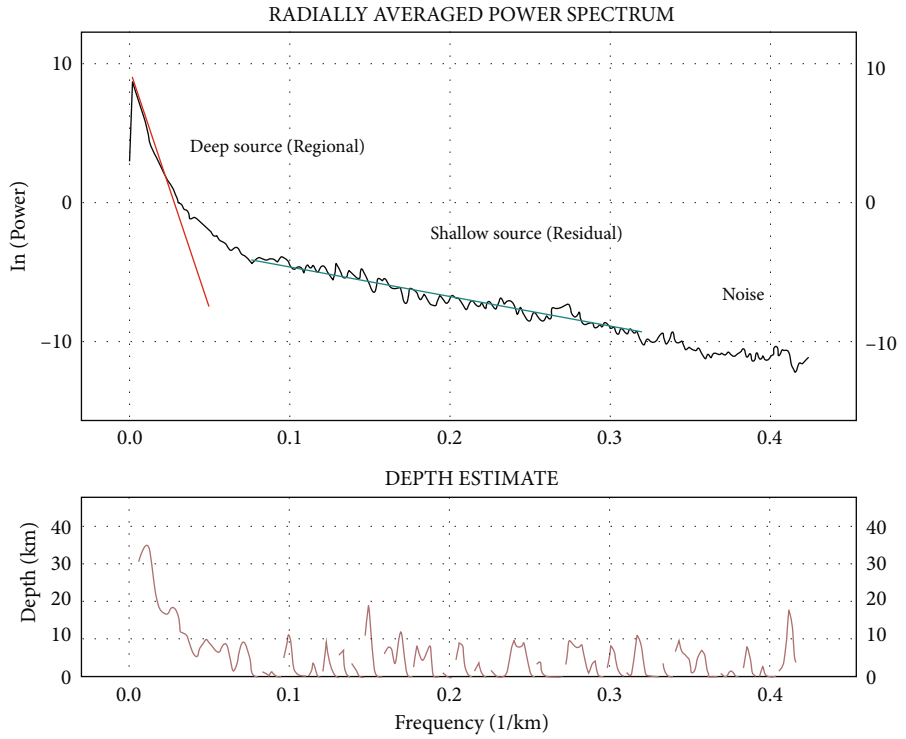

Figure 6: Local power spectrum of RTE magnetic data in the study area.

anomaly. SPI assumes a step-type source model. For a step, the following formula holds:

$$\text{Depth} = \frac{1}{K\ \text{max}}, \tag{2}$$

where K max is the peak value of the local wave number K over the step source.

$$K = \sqrt{\left(\frac{\partial A}{\partial x}\right)^2 + \left(\frac{\partial A}{\partial y}\right)^2}, \tag{3}$$

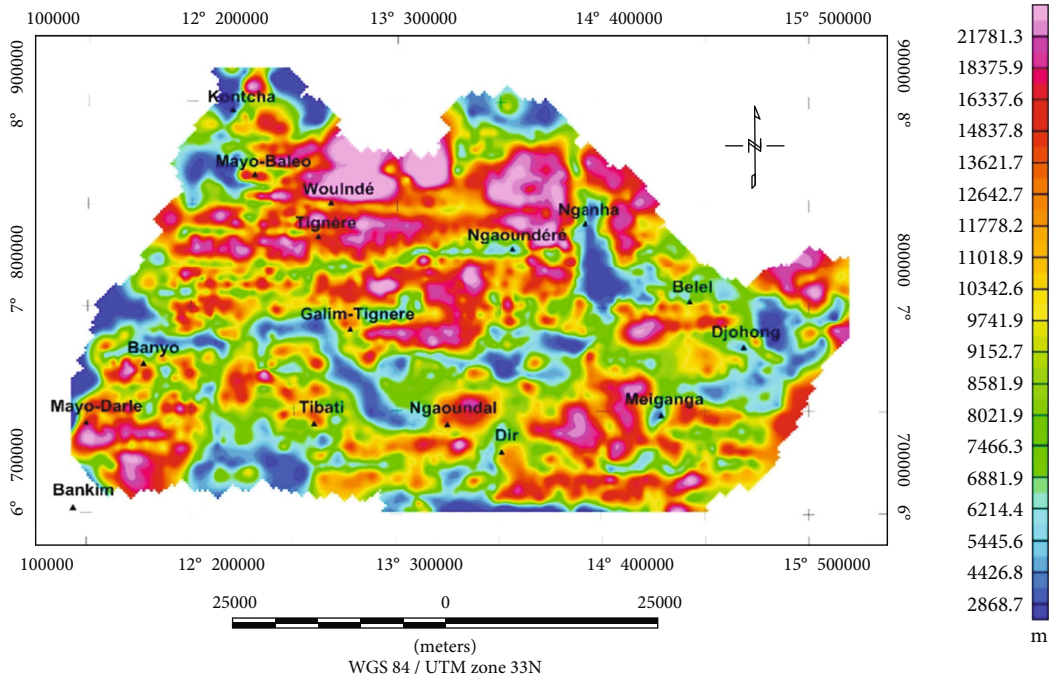

Figure 7: Depth determination from source parameter imaging (SPI).

$$A = \arctan\left(\frac{(\partial M/\partial z)}{\sqrt{(\partial M/\partial x)^2 + (\partial M/\partial y)^2}}\right), \quad (4)$$

where A is the tilt derivative of the total magnetic field anomaly grid M.

SPI module first computes A and K. Then, it finds peak values. These peak values are used to compute depth solutions, which are saved to a database. According to Blakely and Simpson [55], the results may be presented as a grid of depth values (Figure 7).

These methods were applied to RTE for estimating magnetic depths [56]. Its advantage is that the SPI function is an effective, fast, and accurate method. Tested on the real datasets controlled by borehole, its accuracy is +/-20% [57]. Another advantage of this method is that because the method uses the second derivative, the anomaly interference characteristics can be reduced. The SPI solution presented the depths, tilts, and susceptibility contrasts. Thurston and Smith [58] highlight that the depths estimated by SPI solution are not dependent of magnetic declination, inclination, dip, direction, and any residual magnetization. The derived map (SPI) is shown in Figure 7. The highest and lowest SPI was in the range of 22 km and 2 km, respectively. The depth obtained by SPI method corroborates to results of Nnange [49] and Poudjom-Djomani et al. [50].

4.5.2. Depth Calculated by Analytical Signal Technique. Nabighian [59] and Green and Stanly [60] extensively discussed on the 2D analytical signal method for magnetic anomalies in geological model. The model of analytical signal is bell symmetrical on the source body. Their maximum values appear directly at the edges of the source bodies. Also, we can obtain the depths from the form of analytical signals [61]. To obtain the depth by analytic signal method, isocurves are plotted on the analytic signal map. Zero curves are located for each body outline. By simple interpretation of the geometry of anomaly sources, we can estimate depth to top of sources through a table proposed by Macleod et al. [61]. In fact, depths are calculated by measuring the zero contour width of each anomaly accordingly to assume source geometry [61]. The depth by analytical signal in this study (Figure 8) was calculated using the fast Fourier transform tool for RTE anomalies in the frequency domain [62]. This figure shows that these areas have strong contrasts which produce recognizable features on the map. The analytical signal shows the nonuniformity of high magnetization and low magnetization positions in the range of 10-31 km and 0.2-1 km. Therefore, the depth obtained is similar to that of [50].

4.5.3. Forward Modeling. We used the GM-SYS Profile Modeling Module to produce 2D forward models of the geologic structures over the studied region to reveal the subsurface configuration and modeling parameters [19, 63]. Two transects of 2D magnetic models were constructed: profile (AA′) extending about 240 km in a SSW-NNE direction and profile (NN′) extending about 300 km in a WNW-ESE direction (Figure 3). The two 2D forward models produce the representative subsurface geometry and magnetic susceptibility of basement rock. They aid to suggest basement unit in the region based on geologic features.

(1) Profile A-A′. The profile of model A-A′ (Figure 9) is about 200 km long and passes through the west of the study area along the direction of SSW-NNE. The amplitude ranges

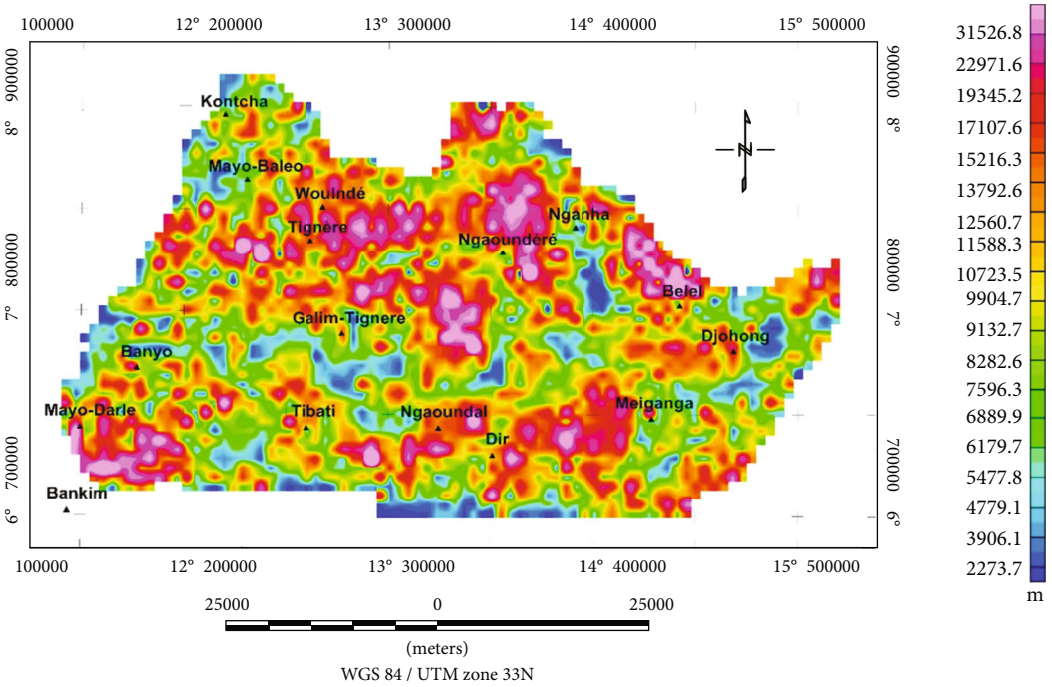

Figure 8: Depth chart of the study area calculated by the analytical signal (AS) method.

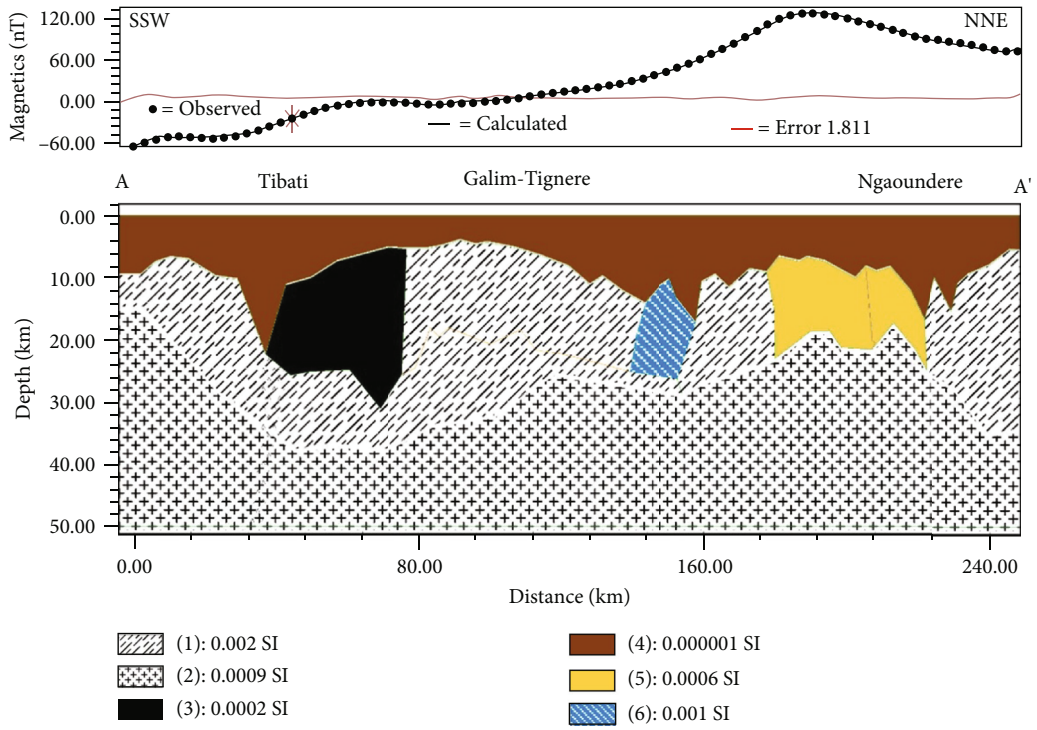

Figure 9: 2D magnetic modeling of A-A′ profile along SSW-NEE direction.

from -60 nT to 120 nT. Positive magnetic anomalies are due to uplift or Horst structures, while negative anomalies are identified in graben or basin structures. The model is divided into three layers, and the underground depth is 2.2–31.5 km. The magnetic susceptibility of the surface layer and the intermediate layer are about 10^{-4} SI and 10^{-3} SI, respectively. Intermediate layer may correspond to amphibole or green schist. This layer contains inclusions with magnetic susceptibility of about 10^{-4} SI, which may be related to granitic basement. Compared with the geological map of the study area, the magnetic susceptibility (0.002SI) of the model is high in Eocene deposits (middle layer) and low in

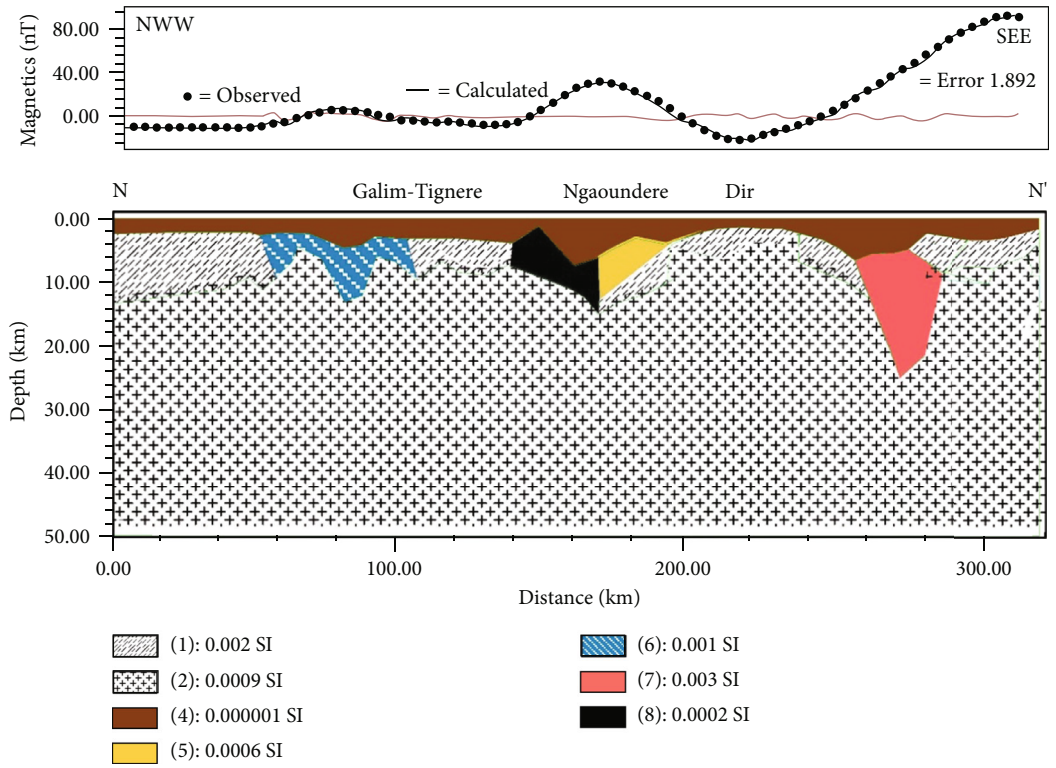

Figure 10: 2D magnetic modeling along N-N′ profile in WNW-ESE direction.

Cretaceous basement and ferruginous, Ferro calcariferous, and intrusions schist.

(2) Profile N-N′. The N-N′ profile of the model (Figure 10) is about 300 km long and passes through the north of the study area along the WNW-ESE direction. The calculated anomaly is completely consistent with the observed anomaly. Positive magnetic anomalies are closely related to uplift or Horst structures, while the large negative magnetic anomalies are related to graben or basin structures. The depth of the underground surface is between 10 and 31.5 kilometers. Compared with the geological map, the model has higher magnetic response to Eocene deposits (west, northwest, east, and northeast) and lower magnetic response to basement (middle) deposits. Therefore, the two profiles are compatible because sand, clay, conglomerate, and clay sandstone represent tertiary to Quaternary sediments, and travertine is located in the middle of each profile.

Geologically, compared with the geological map, the formations obtained in the models are those shown in the geological map, such as incompatible and compatible granites, gabbros, amphiboles, and schists. Structurally, profile A-A′ is parallel to the upper fault, and profile N-N′ is parallel to the structural line on the geological map (Figure 1).

5. Underground Tectonic Inferences

The results and information of the above magnetic data are combined with the geological characteristics in order to determine the main structural characteristics affecting the underground structure in the study area (Figure 11). Therefore, the subsurface consists of a set of faults (primary and secondary) and is inferred from the geological map (Figure 1). The latter direction is N-S, SSW-NNE, and WNW-ESE.

The first fault zone marked in red color is situated on the west and east sides of the study area. This area is locally deep and mainly composed of a series of regional normal faults with NE-SW direction especially in the west of the study area. The second fault zone marked in yellow color is situated in the Midwest of the study area. It highlights shallow structures characterized by the local and regional fault networks in the directions of NE-SW, NW-SE, NS, and ENE-WSW. The third fault zone is located at the southern end of the study area. It is represented in blue color and characterized by acidic magnetic rocks.

Therefore, the whole area is fractured in NE-SW, NW-SE, and N-S directions. These magnetic anomalies are the result of basalt magnetic field fossilization, i.e., residual magnetization. The positive anomaly is due to the magnetization of basalt during cooling, and its direction is consistent with the direction of current field. These anomalies correspond to the local variation of the magnetic field relative to the regional mean field, with strong values (positive anomalies) or weak values (negative anomalies).

Therefore, the mean magnetic field is disturbed by magnetized structures arranged in a parallel direction whose effect adds to or subtracts from the mean magnetic field. It is emphasized that with the reactivation of the Central Cameroon Shear Zone (CCSZ), there is a strong magnetization in

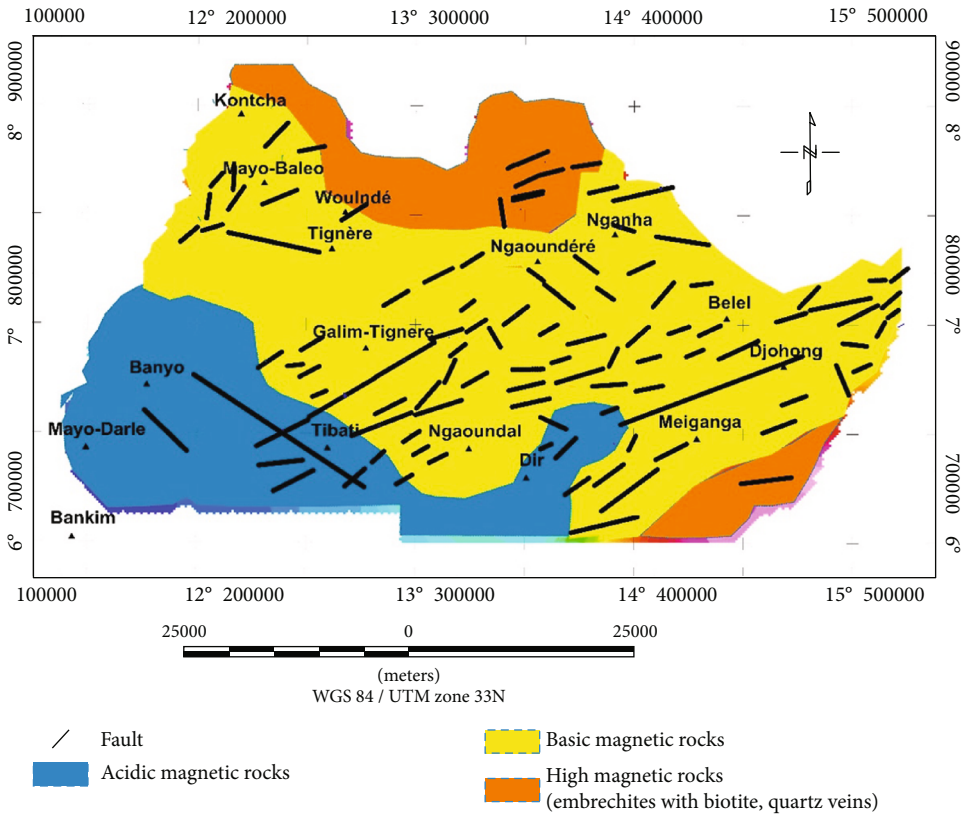

Figure 11: Tectonic map of the magnetic basement from the faults of map from [64].

the granite basement, which is interpreted as an intrusion of volcanic rocks (possibly basalt). The magnetic susceptibility shows that paramagnetic minerals are dominant, as their positive susceptibility values indicate.

6. Conclusion

This study highlights many results which focus on this study and further determines the underground tectonic inference and structural trends in Adamawa region. Equatorial reduction technique is used to directly locate the magnetic anomalies from their causal sources. Therefore, the resulting equatorial reduction map reveals several causal sources and anomalies of different depths and compositions with varying frequency and amplitude. A separation tool has been applied to the reduction to equator map to separate surface anomalies from deep anomalies. Combining the two source methods (imaging parameter method and analytical signal method) is usually the best method to determine various geological constraints including source locations, depths, and thickness (Figures 7 and 8). A 2D modeling tool is used to model profile data, in which more than one anomaly is considered. The models show that the basement rocks are due near vertical faults, which have different projections and dip angles. Therefore, the established basement surface map consists of a group of faults arranged along the N-S, NE-SW, and WNW-ESE directions. In addition, according to various derivation methods (Figure 7), the average depth values of causal points are between 10 and 31 km. From the structural point of view, magnetic methods can basically detect the geometry of underground rocks and structures related to tectonic forces. According to Njeudjang et al. [8], the early characteristics of these areas and the location of springs in the north and northeast of the study area indicate the occurrence of tectonic activity, which may indicate that they may have good geothermal resources.

Data Availability

The magnetic data used to support the findings of this study are included within the article.

Conflicts of Interest

The authors declare that they have no known competing financial interests or personal relationships that could have appeared to influence the work reported in this paper.

Acknowledgments

The authors would like to thank the National Centers for Environmental Information (NCEI) for making the geophysical data used for this research work available to us. The study was funded with personal fund.

References

[1] S. F. Toteu, W. R. Van Schmus, J. Penaye, and A. Michard, "New U-Pb and Sm-Nd data from north-Central Cameroon and its bearing on the pre-Pan African history of Central Africa," *Precambrian Research*, vol. 108, no. 1-2, pp. 45–73, 2001.

[2] S. F. Toteu, J. Penaye, and Y. Poudjom-Djomani, "Geodynamic evolution of the Pan-African belt in central Africa with special reference to Cameroon. Canadian brass Gflatheh Schulzr resistivity profiling with different electrode arrays over a graphite deposit," *Geophysical Prospecting*, vol. 29, pp. 589–600, 1981.

[3] A. Le Maréchal and P. M. Vincent, "Le fossé crétacé du sud Adamaoua (Cameroun)," *Cahiers ORSTOM série-Géologie*, vol. 3, no. 1, pp. 67–83, 1971.

[4] A. Le Maréchal, *Géologie et géochimie des sources thermo minérales du Cameroun*, Thèse Université de Paris VI, 1976.

[5] C. Dorbath, L. Dorbath, J. D. Fairhead, and G. W. Stuart, "A teleseismic delay time study across the central African shear zone in the Adamawa region of Cameroon, West Africa," *Journal of Geophysics and Royal Astronomical Society*, vol. 86, no. 3, pp. 751–766, 1986.

[6] C. S. Okereke, "Contrasting modes of rifting: the Benue trough and Cameroon volcanic line, West Africa," *Tectonics*, vol. 7, no. 4, pp. 775–784, 1988.

[7] Y. H. Poudjom-Djomani, M. Diament, and M. Wilson, "Lithospheric structure across the Adamawa plateau (Cameroon) from gravity studies," *Tectonophysics*, vol. 273, no. 3-4, pp. 317–327, 1997.

[8] K. Njeudjang, J. M. A. Essi, J. D. Kana et al., "Gravity investigation of the Cameroon volcanic line in Adamawa region: geothermal features and structural control," *Journal of African Earth Sciences*, vol. 165, p. 103809, 2020.

[9] P. Kamgang, G. Chazot, E. Njonfang, and F. Tchoua, "Geochimie et geochronologie des roches basiques des monts Bamenda (Cameroun): composition de la source et contamination crustale le long de la ligne volcanique du Cameroun," *Comptes Rendus de Geoscience*, vol. 340, no. 12, pp. 850–857, 2008.

[10] L. Milelli, L. Fourel, and C. Jaupart, "A lithospheric instability origin for the Cameroon volcanic line," *Earth Planet Sciences Letters*, vol. 335-336, pp. 80–87, 2012.

[11] J. Marcel, J. M. A. Essi, J. L. Meli'i, P. N. Nouck, A. Mahamat, and E. Manguelle-Dicoum, "Geodynamic insights of the Cameroon volcanic line (Western Africa) from isostatic gravity anomalies," *Journal of Geodynamics*, vol. 121, pp. 36–48, 2018.

[12] M. G. Dedzo, "Petrology and geochemistry of lavas from Gawar, Minawao and Zamay volcanoes of the northern segment of the Cameroon volcanic line (Central Africa): constraints on mantle source and geochemical evolution," *Journal of African Earth Sciences*, vol. 153, pp. 31–41, 2019.

[13] Y. H. Poudjom-Djomani, *Apport de la gravimétrie à l'étude de la lithosphère continentale et implications géodynamiques. Etude d'un bombement intraplaque: le massif de l'Adamaoua (Cameroun)*, Thèse de Doctorat Université de Paris XI Orsay, France, 1993.

[14] T. C. Noutchogwe, C. T. Tabob, and E. Manguelle-Dicoum, "A gravity study of the crust beneath the Adamawa fault zone, west Central Africa," *Journal of Geophysics and Engineering*, vol. 3, no. 1, pp. 82–89, 2006.

[15] A. O. Ojo, S. Ni, J. Xie, and L. Zhao, "Further constraints on the shear wave velocity structure of Cameroon from joint inversion of receiver function, Rayleigh wave dispersion and ellipticity measurements," *Journal of Geophysics International*, vol. 217, no. 1, pp. 589–619, 2019.

[16] M. E. E. Fosso Téguia, V. G. Nana, and A. S. Lepatio Tchieg, "Exploration of potential ore deposits along the Cameroon volcanic line from gravity and magnetic studies," *Open Journal of Geology*, vol. 10, no. 10, pp. 1009–1026, 2020.

[17] F. E. K. Ghomsi, N. Ribeiro-Filho, R. Baldez et al., "Identification of Cameroon's geological structures through a gravity separation and using seismic crustal models," *Journal of African Earth Sciences*, vol. 173, p. 104027, 2021.

[18] T. C. Noutchogwe, *Investigation géophysique dans la région de l'Adamaoua par les méthodes gravimétriques et magnétiques: implications structurales et hydrogéologiques Thèse de Doctorat/PhD*, vol. 147, Université de Yaoundé I Cameroon, 2010.

[19] Geosoft Program (Oasis Montaj), "Aero Service Company, Mineral Petroleum Groundwater Assessment Program (MAGMAP)," in *2-D frequency-domain processing*, Geosoft Inc Toronto Canada, 2014.

[20] C. Guiraudie, "Carte géologique de reconnaissance à l'échelle du 1/500 000. Feuille Ngaoundéré-Ouest avec notice explicative," *Direction des Mines et de la géologie du Cameroun*, vol. 23, 1955.

[21] M. Lasserre, *Étude géologique de la partie orientale de l'Adamaoua (Cameroun Central) et les principales sources minéralisées de l'Adamaoua*, Bulletin de la Direction des Mines et Géologie du Cameroun n° 4 130 14 fig 6 tabl, 1961.

[22] D. Soba, *La série du Lom: étude géologique et géochronologique d'un bassin volcano-sédimentaire de la chaîne Pan-Africaine de l'Est du Cameroun*, Thèse de Doctorat d'Etat Université de Paris VI 181, 1989.

[23] V. Ngako, P. Jegouzo, and J. P. Nzenti, "Le Cisaillement Centre Camerounais. Rôle structural et géodynamique dans l'orogenèse Pan-Africaine," *Comptes Rendus de l'Académie des Sciences de Paris*, vol. 313, no. 2, pp. 457–463, 1991.

[24] J. P. Nzenti, T. Njanko, and E. T. Njiosseu, "Les domaines granulitiques de la chaîne Pan-Africaine Nord-Equatoriale au Cameroun," *Géologie et Environnement au Cameroun Collection Geocam*, vol. 1, pp. 255–264, 1998.

[25] V. Ngako, "Les déformations continentales Pan-Africaines en Afrique Centrale," in *Résultat d'un poinçonnement de type himalayéen*, Thèse de Doctorat d'État Université de Yaoundé I 241, 1999.

[26] J. P. Nzenti, P. Barbey, and J. M. Bertrand, *La chaîne Pan-Africaine au Cameroun: cherchons suture et modèle*, Abstracts 15eme RST Nancy Société Géologique France édition Paris 99, 1994.

[27] J. P. Nzenti, P. Barbey, and F. M. Tchoua, *Evolution crustale au Cameroun: éléments pour un modèle géodynamique de l'orogenèse néoprotérozoïque*, In: Géologie et environnements au Cameroun Vicat et Bilong, eds Collection Geocam 2, 1999.

[28] T. Ngnotué, J. P. Nzenti, P. Barbey, and F. M. Tchoua, "The Ntui-Betamba high-grade gneisses: a northward extension of the pan-African Yaounde gneisses in Cameroon," *Journal of African Earth Sciences*, vol. 31, no. 2, pp. 369–381, 2000.

[29] B. Kapajika, *Les granites calco-alcalins de l'Ouest de Tibati dans la chaîne Pan-Africaine Nord-équatoriale au Cameroun. Pétrogenèse et structurogenèse*, Thèse de Doctorat Univerité de Lubumbashi 114, 2003.

[30] R. Temdjim, *Le volcanisme de la région de Ngaoundéré (Adamaoua-Cameroun). Étude volcanologique et pétrographique*, Thèse 3e cycle Université Clermont-Ferrand 185, 1986.

[31] J.-M. Dautria and M. Girod, "Les enclaves de lherzolite à spinelle et plagioclase du volcan de Dibi (Adamaoua, Cameroun): des témoins d'un manteau supérieur anormal," *Bulletin Minéral*, vol. 109, no. 3, pp. 275–288, 1986.

[32] A. N. Halliday, A. P. Dickin, A. E. Fallick, and J. G. Fitton, "Mantle dynamics: a Nd, Sr, Pb and O isotopic study of the Cameroon line volcanic chain," *Petrology*, vol. 29, no. 1, pp. 181–211, 1988.

[33] A. Nono, B. Déruelle, D. Demaiffe, and R. Kambou, "Tchabal Nganha volcano in Adamawa (Cameroon): petrology of a continental alkaline lava series," *Jounal of Volcanic Geophysical Research*, vol. 60, no. 2, pp. 147–178, 1994.

[34] J. J. Menard, P. Wandji, and B. Déruelle, "Le volcan de Djinga (Adamaoua-Cameroun): Géologie et Pétrographie," in *Géosciences au Cameroun Collection GEOCAM 1*, J. P. Vicat and P. Bilong, Eds., pp. 169–184, Presse de l'Université de YaoundéI, Cameroon, 1998.

[35] B. Déruelle, I. Ngounouno, and D. Demaiffe, "The 'Cameroon Hot Line' (CHL): a unique example of active alkaline intraplate structure in both oceanic and continental lithospheres," *Comptes Rendus de Geosciences*, vol. 339, no. 9, pp. 589–600, 2007.

[36] D. Soba, A. Michard, and S. F. Toteu, "Données géochronologiques nouvelles (Rb-Sr, U-Pb et Sm-Nd) sur la zone mobile Pan-Africaine de l'Est du Cameroun: âge Protérozoïque supérieur de la série de Lom," *Comptes rendus de l'Académie des sciences. Série 2 Mécanique Physique Chimie Sciences de l'univers Sciences de la Terre*, vol. 312, no. 12, pp. 1453–1458, 1991.

[37] E. Ndjeng, S. E. Belinga, and S. Ngos, *Le secondaire ou Mésozoïque. In: Histoire Géologique du Cameroun*, Géologues du département des Sciences de la Terre de l'Université de Yaoundé I, Les Classiques Camerounais, 2001, Edition Sciences SE Belinga.

[38] R. Temdjim and F. M. Tchoua, "Etude de l'altération palagonitique dans les hyaloclastites du district volcanique de Ngaoundéré (Nord-Cameroun)," *Géologie et environnements au Cameroun Vicat et Bilong eds Collection Geocam*, vol. 2, pp. 285–292, 1999.

[39] A. F. Tiabou, R. Temdjim, P. Wandji et al., "Baossi–Warack monogenetic volcanoes Adamawa Plateau Cameroon: petrography, mineralogy and geochemistry," *Acta Geochim*, vol. 38, no. 1, pp. 40–67, 2019.

[40] Z. Itiga, J. M. Bardintzeff, P. Wotchoko, P. Wandji, and H. Bellon, "Tchabal Gangdaba massif in the Cameroon volcanic line: a bimodal association," *Journal of Geosciences*, vol. 7, no. 11, pp. 4641–4664, 2014.

[41] J. Gouhier and J. D. Nougier, *Contribution à l'étude volcanique du Cameroun ("Ligne du Cameroun"- Adamaoua)*, Annale Faculté des Sciences Yaoundé Cameroun n°17:3-48, 1974.

[42] M. Letterman, *Regional geological study of Anloua basin (Cameroon) Doctorat thesis of 3rd cycle*, Orléans, 1984.

[43] B. Déruelle, J. Ezangono, and J. Lissom, *Mio-Pliocene basaltic lava flows and phonolitic and trachytic plugs north and east of Ngaoundéré (Adamaoua, Cameroon)*, E. Matheis and A. Schandelmeier, Eds., Current Research in African Earth Sciences, Balkema Rotterdam, 1987.

[44] R. Temdjim, I. K. Njilah, P. Kamgang, and C. Nkoumbou, "Données nouvelles sur les laves felsiques de Ngaoundere (Adamaoua, ligne du Cameroun): chronologie K-Ar et petrologie," *Journal of African Sciences Technology*, vol. 5, no. 2, 2006.

[45] A. B. Kampunzu, J. P. H. Caron, and R. T. Lubala, "The east African rift, magma genesis and astheno-lithospheric dynamics," *Geosciences*, vol. 9, no. 4, pp. 211–216, 1986.

[46] R. Langel, G. Ousley, J. Berbert, J. Murphy, and M. Settle, "The MAGSAT mission," *Geophysical Research Letters*, vol. 9, no. 4, pp. 243–245, 1982.

[47] R. D. Regan, J. C. Cain, and W. M. Davis, "A global magmatic anomaly map," *Journal of Geophysical Research*, vol. 80, no. 5, pp. 784–802, 1975.

[48] M. N. Nabighian, "Toward a three-dimensional automatic interpretation of potential field data via generalized Hilbert transforms: fundamental relations," *Geophysics*, vol. 49, no. 6, pp. 780–786, 1984.

[49] J. M. Nnange, *The crustal structure of the Cameroon volcanique line and the Foumban Shear Zone based on gravity and aeromagnetic data*, PhD/thesis University of Leeds England, 1991.

[50] Y. H. P. Djomani, J. M. Nnange, M. Diament, C. J. Ebinger, and J. D. Fairhead, "Effective elastic thickness and crustal thickness variations in West Central Africa inferred from gravity data," *Journal of Geophysical Research: Solid Earth*, vol. 100, no. B11, pp. 22047–22070, 1995.

[51] J. M. Nnange, V. Ngako, J. D. Fairhead, and C. J. Ebinger, "Depths to density discontinuities beneath the Adamawa plateau region, Central Africa, from spectral analyses of new and existing gravity data," *Journal of African Earth Sciences*, vol. 30, no. 4, pp. 887–901, 2000.

[52] S. Nguiya, *Investigation géophysique du bassin volcano-sédimentaire de Lom (Est-Cameroun): implications structurales et tectonique*, Thèse de Doctorat/PhD Université de Yaoundé I, 2009.

[53] M. Dobrin, *Introduction to geophysical prospecting*, McGraw-Hill book Co, New York, Third Edition edition, 1976.

[54] A. Spector and F. S. Grant, "Statistical models for interpreting aeromagnetic data," *Geophysics*, vol. 35, no. 2, pp. 293–302, 1970.

[55] R. J. Blakely and R. W. Simpson, "Approximating edges of source bodies from magnetic or gravity anomalies," *Geophysics*, vol. 51, no. 7, pp. 1494–1498, 1986.

[56] J. D. Phillips, "Locating magnetic contacts: a comparison of the horizontal gradiant, analytical signal and local wavenumber methods," *Society of exploration Geophysicists Abstracts with programs Calagry*, 2000.

[57] A. K. Salako, "Depth to basement determination using source parameter imaging (SPI) of aeromagnetic data: an application to upper Benue trough and Borno Basin north East Nigeria," *Academic Research International*, vol. 5, no. 3, 2014.

[58] J. B. Thurston and R. S. Smith, "Automatic conversion of magnetic data to depth, dip, and susceptibility contrast using the SPI (TM) method," *Geophysics*, vol. 62, no. 3, pp. 807–813, 1997.

[59] M. N. Nabighian, "Additional comments on the analytic signal of two-dimensional magnetic bodies with a polygonal cross-section," *Geophysics*, vol. 39, no. 1, pp. 85–92, 1974.

[60] R. Green and J. M. Stanly, "Application of a HILBERT transform method to the interpretation of surface-vehicle magnetic data," *Geophysical Prospecting*, vol. 23, no. 1, pp. 18–27, 1975.

[61] I. N. MacLeod, K. Jones, and T. F. Dai, "3-D analytic signal in the interpretation of total magnetic field data at low magnetic

latitudes," *Exploration Geophysics*, vol. 24, no. 3-4, pp. 679–687, 1993.

[62] R. J. Blakely, *Potential Theory in Gravity and Magnetic Applications*, Cambridge University Press, 2009.

[63] M. Talwani, G. H. Sutton, and J. L. Worzel, "A crustal section across the Puerto Rico trench," *Journal of Geophysical Research*, vol. 64, no. 10, pp. 1545–1555, 1959.

[64] B. Leroy and A. Cirotteau, *Direction des Mines et de la Géologie Société Nouvelle de Cartographie Lith-Paris*, Projection MTU Méridien International croquis provisoire au 1/200000.S.G.A.E.F Cameroun, 1961.